Molecular Simulation Study of the CO_2-N_2O Analogy

Maximilian Kohns[1], Stephan Werth, Martin Horsch, Erik von Harbou, Hans Hasse

Laboratory of Engineering Thermodynamics, University of Kaiserslautern, Erwin-Schrödinger Str. 44, D-67663 Kaiserslautern, Germany

Abstract

The validity of the CO_2-N_2O analogy concerning the Henry's law constant is investigated by molecular simulation of the solvents water, ethanol, as well as their mixtures. Molecular models for carbon dioxide (CO_2) and for the solvents water and ethanol are taken from the literature. For nitrous oxide (N_2O), two new molecular models are presented. They differ in their structure, but are both parametrized using pure component vapor-liquid equilibrium data. The models are used to study Henry's law constants of CO_2 and N_2O in pure water and pure ethanol over a wide range of temperatures. In the case of water, a slight adjustment in the water-solute interaction is necessary to achieve agreement with experimental data, whereas the gas solubilities in ethanol are predicted quantitatively without any adjustment. For

[1]Author to whom correspondence should be addressed. Electronic mail: maximilian.kohns@mv.uni-kl.de. Telephone: +49-631/205-3216. Fax: +49-631/205-3835.

mixed solvents containing both water and ethanol, the CO_2-N_2O analogy is found to be invalid, contradicting a widespread assumption.
Keywords: CO_2, N_2O, Molecular model, Vapor-liquid equilibrium, Henry's law constant

1. Introduction

The removal of carbon dioxide (CO_2) from gas streams is a common task in many industrial processes. Large scale applications are for example post combustion carbon capture processes and natural gas cleaning. The common process for CO_2 removal is reactive absorption with aqueous solutions of amines as solvents [1, 2]. Upon adsorption, CO_2 reacts with these solvents, forming carbonates and eventually carbamates. CO_2-loaded aqueous amine solutions may show complex phase behavior [3].

In the design of reactive absorption processes, the physical solubility of CO_2 in the solvent is a key property, as it is needed to describe both the phase equilibrium and the chemical equilibrium. A measure of the physical gas solubility is the Henry's law constant $H_{i,j}$ of the solute i in the solvent j. Unfortunately, for reactive systems, this property cannot be determined experimentally in many cases, namely when chemical and physical effects cannot be disentangled in the experiment. Therefore, for reactive systems with

CO_2, the CO_2-N_2O analogy has been established as a workaround [4]. In contrast to CO_2, nitrous oxide (N_2O) normally does not react with the solvents used in reactive absorption processes, so that the Henry's law constant of N_2O in any of these solvents can be determined experimentally using standard methods. Furthermore, the Henry's law constant of both CO_2 and N_2O in pure water is known [5, 6]. In evaluating the Henry's law constant of CO_2 in water, the fact that CO_2 is a weak electrolyte is usually neglected, since the amount of reaction products of CO_2 is very small when the solvent is pure water [7–9]. The CO_2-N_2O analogy assumes that, for a given temperature, the ratio R_H of both gases' Henry's law constants does not depend on the solvent composition, i.e. for aqueous amine solutions:

$$R_\mathrm{H} = \frac{H_{\mathrm{N_2O,water}}}{H_{\mathrm{CO_2,water}}} \stackrel{!}{=} \frac{H_{\mathrm{N_2O,aqueous\ amine\ solution}}}{H_{\mathrm{CO_2,aqueous\ amine\ solution}}} \stackrel{!}{=} \mathrm{const.}, \tag{1}$$

Relying on the validity of Eq. (1), the unknown Henry's law constant of CO_2 in an aqueous amine solution can be determined from the experimental data on the Henry's law constant of N_2O in that solution and the Henry's law constants of both gases in pure water.

The CO_2-N_2O analogy is generally considered to be a practically useful engineering rule [4, 10, 11]. The idea is loosely based on the similarity of the

two molecules CO_2 and N_2O: Both are composed of three atoms, have a linear structure and the same molecular mass [12]. Furthermore, many pure component properties of CO_2 and N_2O, such as the vapor pressure, the saturated liquid and vapor density, and the enthalpy of vaporization, are similar, but not completely identical [13, 14]. However, these similarities in the pure component properties do not imply that their behavior in mixtures is similar as well. Nevertheless, the CO_2-N_2O analogy assumes that a non-reacting CO_2 molecule is similar to a N_2O molecule when gas solubilities in various solvents are considered.

As an alternative to experimental studies, molecular simulation can be used to study phase equilibria. When carried out properly, the quality of the simulation results solely depends on the quality of the employed molecular models. In this work, a simple approach for assessing the validity of the CO_2-N_2O analogy based on molecular simulation is presented. It is explored for the solvents water, ethanol, and their mixtures. Using molecular simulation, the Henry's law constants of CO_2 and N_2O are predicted for the pure solvents and their mixtures and the validity of the CO_2-N_2O analogy is assessed. The solvent ethanol is chosen here because experimental data on the solubility of both gases in ethanol are available in the literature [15–17]. The

reactions of CO_2 with ethanol are negligible, as they are for water, and also N_2O does not react with ethanol. Additionally, experimental data also exist in the literature for the solubility of CO_2 in mixtures of water and ethanol [17]. In molecular simulations, only physical effects are considered. Hence, even when a mixture is modeled in which CO_2 would react, e.g. an aqueous amine solution, the reactions are neglected and only the physical solubility is studied in the simulations.

A number of molecular simulation studies have been carried out for determining the solubilities of CO_2 in various solvents [18–25], whereas N_2O has drawn much less attention [25]. There is a large number of CO_2 models available in the literature, some of which describe the VLE of pure CO_2 reasonably well. For a detailed discussion, see the recent paper of Jiang et al. [26]. In contrast, there are only three N_2O models available to date [27–29], and none of them is able to describe the VLE with satisfactory accuracy. Therefore, two new molecular models for N_2O are developed in the present work, which differ in their structure, but are parametrized using the same data.

2. Molecular Models and Simulation Methods

2.1. Molecular Models

All molecular models used in the present study are rigid and non-polarizable. They contain Lennard-Jones (LJ) sites to describe dispersion and repulsion and partial charges or point quadrupoles to account for hydrogen bonding and polarity. Therefore, all potentials can be written as special cases of

$$
\begin{aligned}
U &= U_{\mathrm{LJ}} + U_{\mathrm{CC}} + U_{\mathrm{CQ}} + U_{\mathrm{QQ}} \\
&= \sum_{i=1}^{N-1} \sum_{j=i+1}^{N} \left\{ \sum_{a=1}^{n_i^{\mathrm{LJ}}} \sum_{b=1}^{n_j^{\mathrm{LJ}}} 4\epsilon_{ijab} \left[\left(\frac{\sigma_{ijab}}{r_{ijab}} \right)^{12} - \left(\frac{\sigma_{ijab}}{r_{ijab}} \right)^{6} \right] \right. \\
&\quad + \sum_{c=1}^{n_i^e} \sum_{d=1}^{n_j^e} \frac{1}{4\pi\varepsilon_0} \left[\frac{q_{ic} q_{jd}}{r_{ijcd}} + \frac{q_{ic} Q_{jd} + q_{jd} Q_{ic}}{r_{ijcd}^3} f_1(\omega_i, \omega_j) \right. \\
&\quad \left. \left. + \frac{Q_{ic} Q_{jd}}{r_{ijcd}^5} \cdot f_2(\omega_i, \omega_j) \right] \right\}. \qquad (2)
\end{aligned}
$$

Here, a, b, c and d denote sites, i and j denote molecules. ε_0 is the vacuum permittivity, ϵ_{ijab} and σ_{ijab} are the Lennard-Jones energy and size parameters, r_{ijab} and r_{ijcd} are site-site distances, q_{ic}, q_{jd}, Q_{ic} and Q_{jd} are the magnitude of the point charges and quadrupole moments, respectively. Moreover, $f_1(\omega_i, \omega_j)$ and $f_2(\omega_i, \omega_j)$ are dimensionless angle-dependent expressions

in terms of the orientation (ω_i,ω_j) of the electrostatic interaction sites [30]. The modified Lorentz-Berthelot combining rules are used [31, 32] for the interaction between unlike Lennard-Jones sites

$$\sigma_{ijab} = \frac{\sigma_{iiaa} + \sigma_{jjbb}}{2}, \tag{3}$$

$$\epsilon_{ijab} = \xi_{ij}\sqrt{\epsilon_{iiaa}\epsilon_{jjbb}}. \tag{4}$$

The adjustment of a binary interaction parameter ξ_{ij} is only necessary for the systems 'water + CO_2' and 'water + N_2O' (cf. Section 3.2). Hence, the original Lorentz-Berthelot combining rules are retained in all other cases, i.e. $\xi_{ij} = 1$ for 'water + ethanol' as well as 'ethanol + CO_2' and 'ethanol + N_2O'. The molecular models for the two solvents water and ethanol are taken from the literature: the water model is TIP4P/2005 [33], and the ethanol model is taken previous work of our group [20]. Both models have been used successfully in several molecular simulation studies [34–38].

For CO_2, two different models are assessed, which are taken from previous work of our group. The model of Vrabec et al. [39] uses the two center Lennard-Jones plus quadrupole approach (2CLJQ), employing two equal LJ sites and a point quadrupole in the center of mass. The model of Merker et al. [40] employs two equal LJ sites for the oxygen atoms and a different LJ

site for the central carbon atom, while also describing the electrostatic interactions with a point quadrupole in the center of mass. This model is denoted as 3CLJQ in the present work. Both models show almost equal performance in the VLE of pure CO_2 and have also been applied successfully in studies of mixtures [20, 22–24].

Inspired by the general idea of the CO_2-N_2O analogy, two new molecular models for N_2O were developed in the present work. They follow the same modeling approaches as their CO_2 counterparts: One model is of the 2CLJQ type, and the other model is of the 3CLJQ type. In the latter one, the LJ sites for both nitrogen atoms are equal, while the LJ site for oxygen is different from these two. In both cases, the point quadrupole is located in the center of mass. The structure of the two new models and that of the literature models in shown schematically in Fig. 1.

Both models were optimized with respect to the VLE of pure N_2O in the temperature range $201 \leq T\ /\ \mathrm{K} \leq 296$, corresponding to $0.65 \leq\ T\ /\ T_\mathrm{c}\ \leq 0.95$. Two objectives were considered: the mean relative deviations in the vapor pressure and in the saturated liquid density. As a reference, the equation of state (EOS) of Lemmon and Span [14] was used. Correlations of VLE properties of the 2CLJQ model are available as functions of the four model

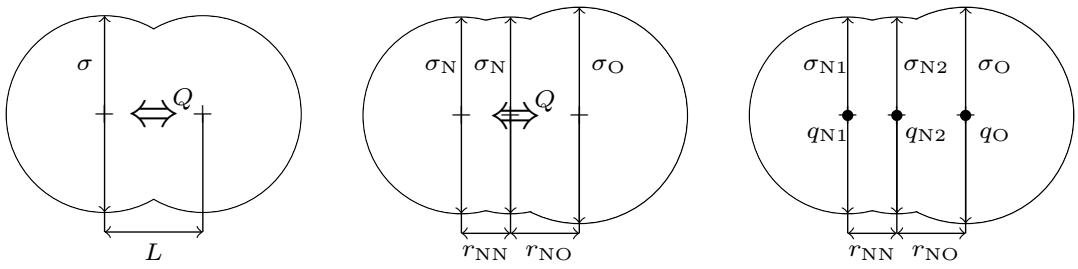

Figure 1: Structure of molecular models for nitrous oxide, schematically. Left: 2CLJQ model developed in this work. Middle: 3CLJQ model developed in this work. Right: models from the literature [27–29]. LJ sites are shown by crosses, double arrows indicate the locations of point quadrupoles, dots show partial charges. For the nitrous oxide model of Costa Gomes et al. [27], the LJ sites for N1 and N2 are equal, whereas they are different in the models of Hansen et al. [28] and Lachet et al. [29]. Note that these sketches are not in actual scale in order to emphasize the differences between the models.

parameters [41]. Therefore, the parametrization of 2CLJQ models can be carried out efficiently, even when advanced techniques like the Pareto approach by Stöbener et al. are used [42]. This was done here and the Pareto set of a 2CLJQ model of N_2O was determined, using the two objective functions given above. Furthermore, one model in the Pareto knee was selected, which is a good compromise between the two objectives. Molecular simulations were then carried out to check the model quality, and a slight further improvement could be achieved by the reduced units method of Merker et al. [43].

For the 3CLJQ model, a conventional parameter optimization using a Newton scheme was performed as proposed by Eckl et al. [44] with respect to the saturated liquid density and the vapor pressure. As in the 2CLJQ case, further fine-tuning of the model using the reduced units method by Merker et al. [43] was accomplished. The parameters of the two new molecular models for N_2O are presented in Table 1.

2.2. Simulation Methods

The VLE of pure N_2O was computed with the Grand Equilibrium method of Vrabec and Hasse [45]. To assess the predictive capability of the models, the surface tension of pure N_2O was computed in MD simulations using the

Table 1: Parameters of the new molecular models for nitrous oxide. For the 3CLJQ model, both LJ sites representing nitrogen are identical. The point quadrupole is located in the center of mass for both models.

2CLJQ		3CLJQ	
σ / Å	3.0503	σ_{N} / Å	3.0802
ϵ/k_{B} / K	133.7920	$\epsilon_{\mathrm{N}}/k_{\mathrm{B}}$ / K	46.4285
		σ_{O} / Å	3.0612
		$\epsilon_{\mathrm{O}}/k_{\mathrm{B}}$ / K	88.2224
L / Å	2.2688	r_{NN} / Å	1.1316
		r_{NO} / Å	1.1877
Q / DÅ	3.6810	Q / DÅ	3.7657

methods described by Werth et al. [46]. The Henry's law constant of a solute i (either CO_2 or N_2O) in the solvent *solv* (either water, ethanol, or a mixture of both) was obtained by sampling the chemical potential of the solute i at infinite dilution μ_i^∞ and using the relation [47]

$$H_{i,solv}(T) = \rho_{solv} RT \ \exp\left(\mu_i^\infty / k_\mathrm{B} T\right), \tag{5}$$

where k_B is Boltzmann's constant, R is the universal gas constant, and ρ_{solv} is the density of the solvent, which can be computed on the fly. The statistical uncertainty of Henry's law constant was estimated by evaluating the standard deviation of μ_i^∞ with the block averaging method of Flyvbjerg and Petersen [48]. The upper and lower limits for Henry's law constant were obtained by computing it from μ_i^∞ plus or minus three standard deviations. All simulations of the present study were carried out with the molecular simulation programs *ms2* [49] and, for the simulation of the surface tension, *ls1 mardyn* [50]. Technical simulation details are given in the Appendix, and all numerical simulation results of this work are tabulated in the Supplementary Material.

3. Results and Discussion

3.1. Molecular Models for Nitrous Oxide

The VLE of the two new molecular models for N_2O is compared to the EOS by Lemmon and Span [14] in Fig. 2.

Both models perform almost equally well for the VLE of pure N_2O. The critical properties were derived from the simulation results using the procedure proposed by Lotfi et al. [51] and agree favorably with the EOS critical properties, cf. Table 2. For the comparison of the performance of the two new models for N_2O with existing models from the literature, deviation plots of the VLE properties are shown in Fig. 3, and the mean deviations from the EOS data are presented in Table 3.

For the liquid and vapor densities, the two new models perform equally well as the best literature model, which is that of Hansen et al. [28]. For the vapor pressure, the two new models yield better results than the existing ones. For the enthalpy of vaporization, the two new models are similar to the model of Hansen et al. [28], whereas the Lachet et al. [29] model yields the best results.

Additionally, the Pareto front obtained for the 2CLJQ model is shown in Fig. 4 together with the deviations in ρ_l and p^s of all N_2O models.

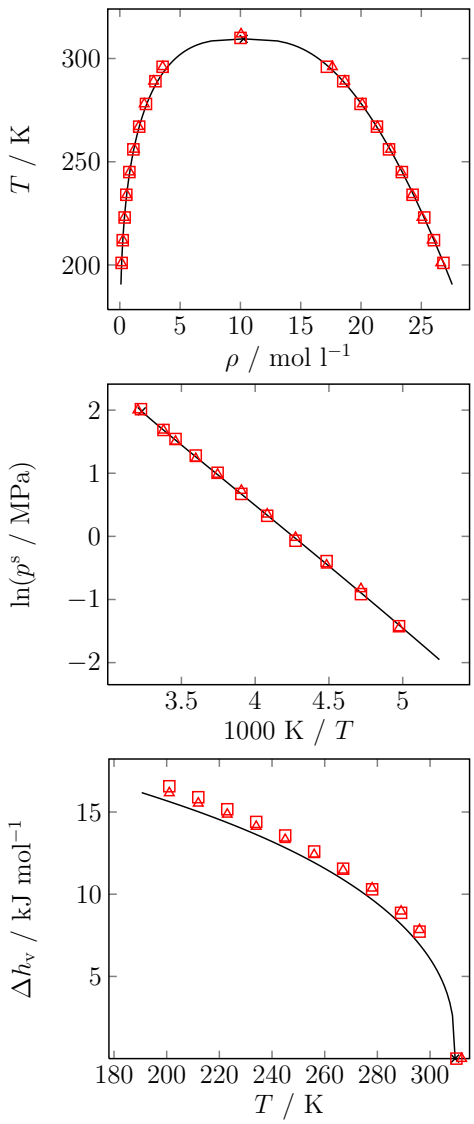

Figure 2: Vapor-liquid equilibrium of the two new molecular models for nitrous oxide. Simulation results for the 2CLJQ model (□) and the 3CLJQ model (△) are compared to the equation of state by Lemmon and Span [14] (–, the cross represents the critical point). Top panel: Saturated liquid and vapor densities. Middle panel: vapor pressure. Bottom panel: enthalpy of vaporization. Statistical uncertainties are within symbol size.

Table 2: Critical properties of N_2O as predicted by various molecular models compared to critical properties of the EOS of Lemmon and Span [14].

Model	T_c / K	p_c / MPa	ρ_c / mol l^{-1}
EOS [14]	309.5	7.25	10.27
Costa Gomes et al. [27]	323.7	7.69	9.79
Hansen et al. [28]	308.8	7.61	10.17
Lachet et al. [29]	304.7	7.47	10.25
2CLJQ, this work	310.0	7.52	10.01
3CLJQ, this work	311.8	7.38	10.05

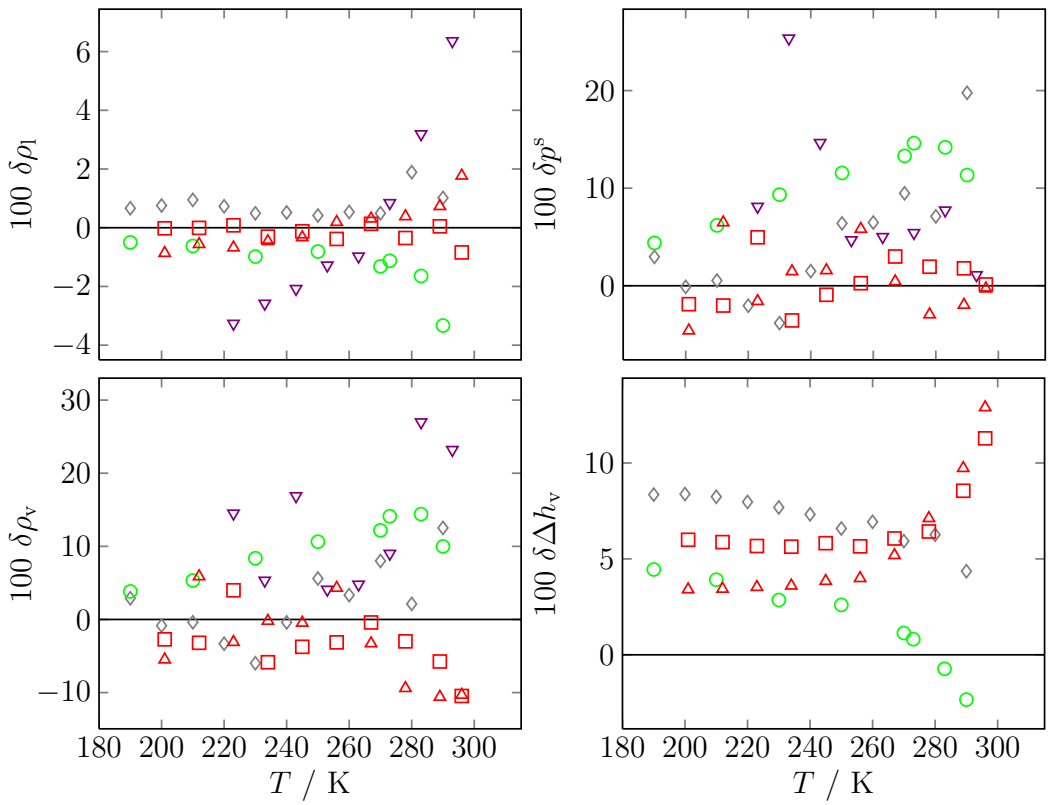

Figure 3: Relative deviations between simulation results and the EOS by Lemmon and Span [14], defined as $\delta z = (z_{\mathrm{Sim}} - z_{\mathrm{EOS}})/z_{\mathrm{EOS}}$ for the VLE of nitrous oxide. Left panel: saturated liquid and vapor densities, right panel: vapor pressure and enthalpy of vaporization. Symbols correspond to different molecular models for nitrous oxide: this work 2CLJQ (□), this work 3CLJQ (△), Costa Gomes et al. [27] (▽), Hansen et al. [28] (◇), Lachet et al. [29] (○). The results for the molecular models from the literature were taken from the original publications. No data for the enthalpy of vaporization was given by Costa Gomes et al. [27]. Statistical uncertainties are not shown for the sake of clarity.

Table 3: Mean relative deviations between simulation results and the EOS by Lemmon and Span [14], defined as $\delta z = |(z_{\mathrm{Sim}} - z_{\mathrm{EOS}})/z_{\mathrm{EOS}}|$ for VLE properties of nitrous oxide. The results for the molecular models from the literature were taken from the original publications. No data for the enthalpy of vaporization was given by Costa Gomes et al. [27].

	Costa Gomes et al. [27]	Hansen et al. [28]	Lachet et al. [29]	2CLJQ	3CLJQ
ρ_{l}	2.6%	0.8%	1.3%	0.2%	0.6%
ρ_{v}	13.1%	4.1%	9.9%	4.2%	5.3%
p^{s}	9.0%	5.5%	10.6%	2.2%	2.7%
Δh_{v}	–	7.1%	2.4%	6.7%	5.7%

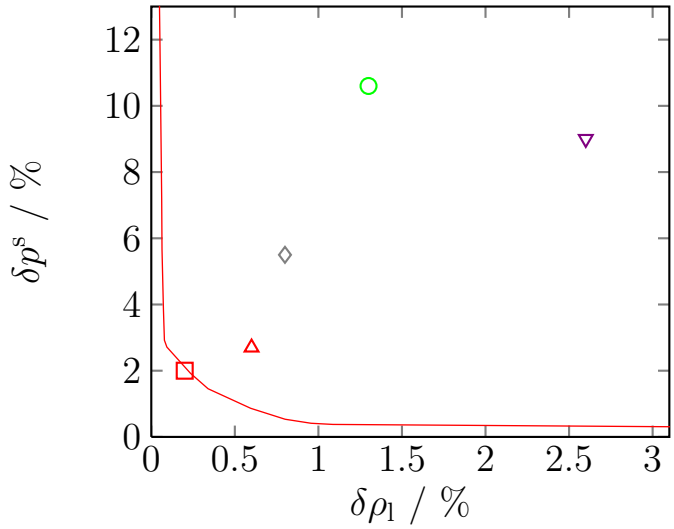

Figure 4: Pareto front for 2CLJQ models for nitrous oxide (–) and deviations of molecular models from the EOS by Lemmon and Span [14]. Symbols correspond to different molecular models for nitrous oxide: this work 2CLJQ (□), this work 3CLJQ (△), Costa Gomes et al. [27] (▽), Hansen et al. [28] (◇), Lachet et al. [29] (○).

The chosen 2CLJQ model lies in the region of the Pareto knee on the front. The 3CLJQ model, although more complex, does not attain the quality of the 2CLJQ model. This is not astonishing because the 3CLJQ model is asymmetric, whereas real N_2O is almost symmetric due to its mesomery [12]. Even the best literature model is clearly worse than the models developed here regarding the deviations in ρ_{l} and p^{s}. It is remarkable that the 2CLJQ model (4 parameters) outperforms the 3CLJQ model (7 parameters) and the literature models employing partial charges (8 parameters for the model of

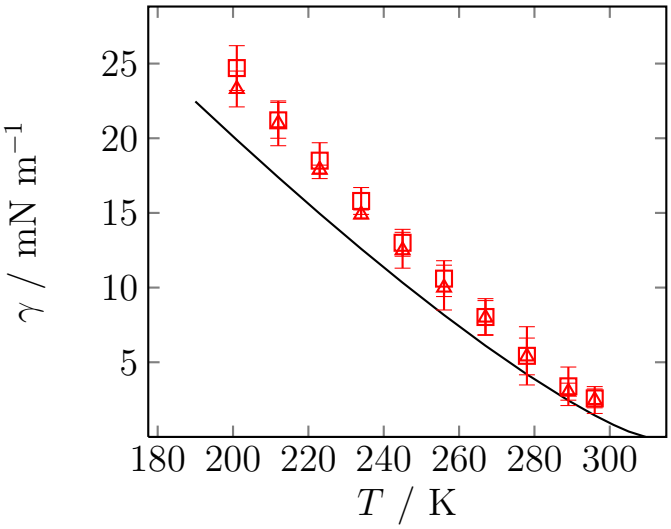

Figure 5: Surface tension of the two new molecular models for nitrous oxide. Simulation results for the 2CLJQ model (□) and the 3CLJQ model (△) are compared to the DIPPR correlation [52] (–).

Costa Gomes et al. [27], and 10 parameters for the other two literature models [28, 29]), even though it is conceptually much simpler and computationally more efficient.

As a further test of the quality of the two new molecular models for N_2O, the vapor-liquid surface tension was computed for both models. In Fig. 5, the simulation results are compared to a correlation of experimental data from the DIPPR database [52].

Both models overestimate the surface tension of pure N_2O. However, the trend is captured accurately and the deviations are less pronounced for higher

temperatures. On average, the surface tension is overestimated by about 25 % (2CLJQ) and 20 % (3CLJQ), which are typical values for molecular models of real fluids which were parametrized to VLE data [53].

In summary, the two new molecular models for N_2O capture the pure fluid properties well. In the following section, it is shown that also reliable data on mixtures can be obtained with these models.

3.2. Assessment of the Analogy

In order to assess the model performance – not only of the solutes but also of the solvents – simulations of Henry's law constants of both gases in the pure solvents water and ethanol were carried out over a wide range of temperatures. Fig. 6 shows the results for pure water as the solvent, modeled by TIP4P/2005 [33]. It is combined with all four solute models: the 2CLJQ CO_2 model by Vrabec et al. [39], the 3CLJQ CO_2 model by Merker et al. [40], and the two new models for N_2O from the present work.

As the predictions using the original Lorentz-Berthelot combining rules (i.e. $\xi_{ij} = 1$) lead to an important overestimation of Henry's law constant in all cases, a binary interaction parameter ξ_{ij} was adjusted, cf Eq. (4). It was adjusted to yield the correct Henry's law constant of the respective solute model in TIP4P/2005 water at a temperature of 313.15 K, using the cor-

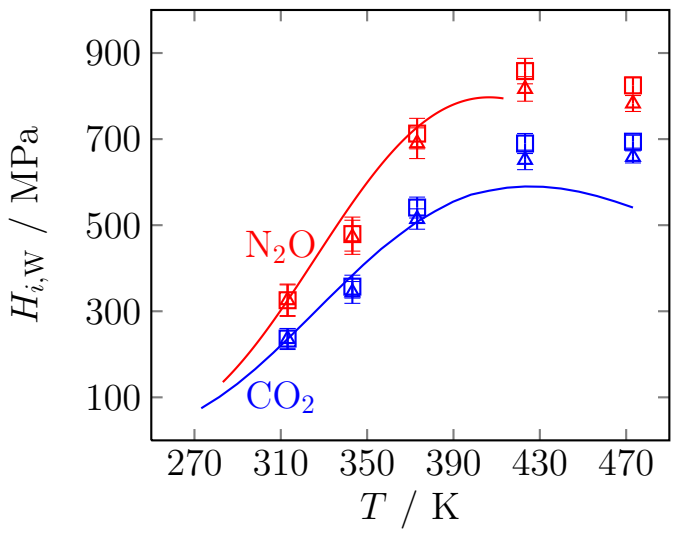

Figure 6: Henry's law constant of N_2O and CO_2 in pure water as a function of the temperature. Simulation results for N_2O (□ 2CLJQ this work, △ 3CLJQ this work) and CO_2 (□ 2CLJQ Vrabec et al. [39], △ 3CLJQ Merker et al. [40]) are compared to correlations of experimental data for N_2O of Penttilä et al. [6] (–) and for CO_2 of Rumpf and Maurer [5] (–). Binary interaction parameters $\xi_{i,\mathrm{W}}$ were fit to $H_{i,\mathrm{W}}(T = 313.15\ \mathrm{K})$ given by the correlations.

Table 4: Binary interaction parameters adjusted in this work to the Henry's law constant of N_2O and CO_2 in pure water at $T = 313.15$ K.

Solute model	$\xi_{i,\mathrm{TIP4P/2005}}$
N_2O, 2CLJQ	1.0466
N_2O, 3CLJQ	1.0434
CO_2, 2CLJQ [39]	1.0748
CO_2, 3CLJQ [40]	1.0608

relations of Penttilä et al. [6] and Rumpf and Maurer [5] as the reference. With this adjusted value of the temperature-independent interaction parameter ξ_{ij}, the temperature dependence of Henry's law constant is predicted reasonably well by all four model combinations. The Henry's law constant is only overestimated in the high temperature region, but the fact that it has a maximum is predicted correctly. The optimized interaction parameters are given in Table 4. The same systematic investigation was conducted for the solvent ethanol. The Henry's law constants of all four solute models together with the ethanol model of Schnabel et al. [20] are presented in Fig. 7, where

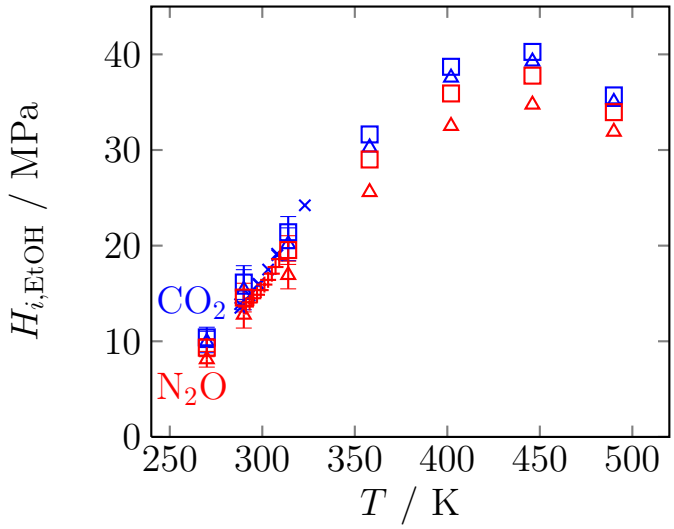

Figure 7: Henry's law constant of N_2O and CO_2 in pure ethanol as a function of the temperature. Simulation results for N_2O (□ 2CLJQ this work, △ 3CLJQ this work) and CO_2 (□ 2CLJQ Vrabec et al. [39], △ 3CLJQ Merker et al. [40]) are compared to experimental data for N_2O (+) [15] and for CO_2 (×) [16, 17]. Simulation uncertainties are only shown explicitly where they exceed the symbol size.

they are compared to a compilation of experimental data points from the literature.

In the case of ethanol, as opposed to water, the predictions of all the model combinations fit well with the experimental data in the narrow temperature range in which such data are available for a comparison. Therefore, the original Lorentz-Berthelot combining rules ($\xi_{ij} = 1$) were retained. The system '2CLJQ CO_2 + ethanol' has already been considered by Schnabel et al. [20],

who adjusted a binary interaction parameter of $\xi_{CO_2,EtOH} = 0.992$, which is very close to 1. Here, we prefer to rely on the predictive capability of the models and therefore refrain from making this slight adjustment.

Fig. 7 shows that the differences between the two studied CO_2 models regarding the Henry's law constants in ethanol are small. For the two N_2O models, somewhat higher differences are observed at high temperatures. The results discussed above show that, where experimental data are available, the differences between the alternative models are small. However, for N_2O the 2CLJQ and for CO_2 the 3CLJQ model are slightly better than their corresponding alternatives. Therefore, the following investigation of mixed solvents is restricted to the two solute models 2CLJQ N_2O and 3CLJQ CO_2. Preliminary simulations which we have carried out with the other solute models and which are not documented here show that this choice has no influence on the main conclusion from the study.

On this basis, 'water + ethanol' mixed solvents were considered at different compositions and $T = 323.15$ K. The results are shown in Fig. 8.

For the solute CO_2, experimental data are available in the mixed solvent from Dalmolin et al. [17] and the model predictions are in good agreement with these data. No experimental data on the solubility of N_2O in the mixed

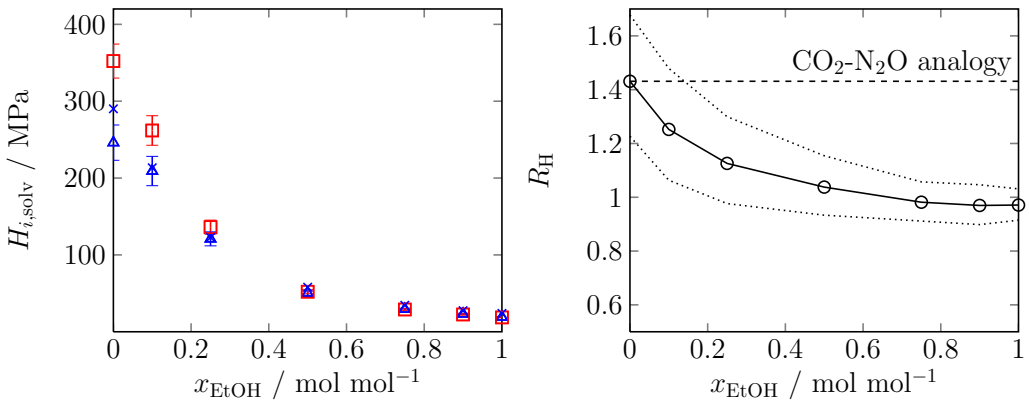

Figure 8: Henry's law constant of N_2O and CO_2 over the gas-free solvent composition in water + ethanol mixed solvents at $T = 323.15$ K. Left panel: Simulation results for the 2CLJQ N_2O model (□) and the 3CLJQ CO_2 model [40] (△) are compared to experimental data for CO_2 of Dalmolin et al. [17] (×). Right panel: Ratio of Henry's law constants $R_{\mathrm{H}} = H_{\mathrm{N_2O},solv}/H_{\mathrm{CO_2},solv}$ from molecular simulation (○), the solid line is a guide to the eye. The dotted lines show the confidence band estimated from the uncertainties in the simulated Henry's law constants. The dashed line shows the constant ratio assumed in the CO_2-N_2O analogy.

solvent are available. This gap is closed by the present molecular simulations. The right panel of Fig. 8 shows the ratio of Henry's law constants R_{H}, cf. Eq. (1), as a function of the solvent composition. Adding ethanol to water results in a sharp drop of the ratio R_{H}. Only in the ethanol-rich region, this ratio R_{H} is approximately constant. Clearly, the CO_2-N_2O analogy is not valid for the investigated solvent mixture water + ethanol. This is confirmed also by the experimental Henry's law constant ratios in the pure solvents alone: The ratio is found to be $R_{\mathrm{H}} \approx 1.4$ in water, whereas it is $R_{\mathrm{H}} \approx 1.0$ in ethanol. The present simulations show that the analogy already breaks down for small mole fractions of ethanol in water, sooner than one would have expected based on these data alone.

4. Conclusion

Two new molecular models for nitrous oxide, a 2CLJQ and a 3CLJQ model, were developed. Both models describe the VLE of nitrous oxide equally well, and are in better agreement with the reference equation of state than any literature model available to date. The two models also provide reliable results for the Henry's law constants of nitrous oxide in the two pure solvents water and ethanol. The same was found for the 2CLJQ model

of Vrabec et al. [39] and the 3CLJQ model of Merker et al. [40] for carbon dioxide. An adjustment of the binary interaction gas-solvent is only necessary for water, whereas gas solubilities in ethanol are predicted quantitatively without considering binary data.

The successful study of the solubility of CO_2 and N_2O in the pure solvents was the basis for an investigation of ternary systems. Using molecular simulation, it was shown that the CO_2-N_2O analogy is invalid for the solvent mixture water + ethanol. The methodology presented here can be used to study other systems relevant for carbon dioxide removal from gas streams in future work. The high quality of the results of the molecular simulations found in the present work indicates that physical gas solubilities in reactive solvents can be predicted reliably by molecular models.

Acknowledgments

The present work was conducted under the auspices of the Boltzmann-Zuse Society of Computational Molecular Engineering (BZS) and the simulations were carried out on the Regional University Computing Center Kaiserslautern (RHRK) under the grant TUKL-MSWS, the High Performance Computing Center Stuttgart (HLRS) under the grant MMHBF as

well as the Leibniz Supercomputing Centre (LRZ) under the grant SPARLAMPE (pr48te). The authors thank Stephan Deublein and Steffen Reiser for fruitful discussions.

Funding

This work was supported by the Reinhart Koselleck Program (HA1993/15-1) of the German Research Foundation (DFG).

Appendix A. Simulation Details

In all simulations of the present study, electrostatic long-range interactions were calculated using the reaction field method [54] and the temperature was kept constant using a velocity scaling thermostat. In all molecular dynamics (MD) simulations, the time step was 1.2 fs.

Appendix A.1. VLE of Pure Nitrous Oxide

For the VLE of pure nitrous oxide, the Grand Equilibrium method by Vrabec and Hasse [45] was used. First, the chemical potential of pure nitrous oxide in the liquid phase was sampled with Widom's test particle insertion in MD simulations in the NpT ensemble, using 1372 particles and Berendsen's barostat. The cutoff radius was 19.5 Å. The fluid was equilibrated for

25000 time steps, before sampling was carried out for 200000 time steps. Up to 5000 test particles were inserted every time step. Then, the vapor phase was simulated in a pseudo-μVT ensemble Monte Carlo (MC) simulation, in which equilibration and production took 20000 and 50000 MC loops, respectively. Each loop consisted of $N_{\mathrm{NDF}}/3$ steps, where N_{NDF} indicates the total number of mechanical degrees of freedom of the system, plus two insertion and deletion attempts. The cutoff radius was equal to half the box length.

Appendix A.2. Henry's Law Constant

Henry's law constant was sampled according to Eq. (5) of the main text. MD simulations were carried out with 1000 solvent molecules in the NpT ensemble at pressures close to the vapor pressure of the pure solvent at the respective temperature. The chemical potential of the solute was sampled with Widom's test particle insertion, again with up to 5000 trial insertions per time step. Equilibration and production took 50000 and 1000000 time steps, respectively, and the cutoff radius was 15.5 Å.

Appendix A.3. Surface Tension

The surface tension of pure N_2O was computed in MD simulations with the approach of Werth et al. [46]. The simulations were carried out in the

NVT ensemble, and equilibration and production took 500000 and 2500000 time steps, respectively. The cutoff radius was 19.5 Å.

Nomenclature

Abbreviations

2CLJQ	Two center Lennard-Jones plus quadrupole
3CLJQ	Three center Lennard-Jones plus quadrupole
EOS	Equation of state
EtOH	Ethanol
LJ	Lennard-Jones
MC	Monte Carlo
MD	Molecular dynamics
VLE	Vapor-liquid equilibrium
W	Water

Symbols

γ	Vapor-liquid surface tension
ϵ	LJ energy parameter
ε_0	Vacuum permittivity
f_1, f_2	Angle-dependent functions

Δh_{v}	Enthalpy of vaporization
$H_{i,j}$	Henry's law constant of solute i in solvent j
k_{B}	Boltzmann's constant
L	Elongation
μ_i	Chemical potential of component i
n	Number of sites
N	Number of molecules
ω	Angle
p	Pressure
q	Point charge
Q	Quadrupole moment
ρ	Density
r	Distance
R	Universal gas constant
R_{H}	Ratio of Henry's law constants
σ	LJ size parameter
T	Temperature
U	Potential
V	Volume

ξ_{ij}	Binary interaction parameter
x	Mole fraction

Subscripts and Superscripts

a, b, c, d	Site index
c	Critical
e	Electrostatic
i, j	Component / molecule index
l	Saturated liquid
N	Nitrogen
O	Oxygen
s	Saturated
solv	Solvent
v	Saturated vapor
∞	At infinite dilution

References

[1] R. Notz, I. Tönnies, N. McCann, G. Scheffknecht, H. Hasse, CO_2 Capture for Fossil Fuel-Fired Power Plants, Chem. Eng. Technol. 34 (2011) 163–172. doi:10.1002/ceat.201000491.

[2] M. Wang, A. Lawal, P. Stephenson, J. Sidders, C. Ramshaw, Post-combustion CO_2 Capture with Chemical Absorption: A State-of-the-art Review, Chem. Eng. Res. Des. 89 (2011) 1609–1624. doi:10.1016/j.cherd.2010.11.005.

[3] D. Vasiliu, A. Yazdani, N. McCann, M. Irfan, R. Schneider, J. Rolker, G. Maurer, E. von Harbou, H. Hasse, Thermodynamic Study of a Complex System for Carbon Capture: Butyltriacetonediamine + Water + Carbon Dioxide, J. Chem. Eng. Data 61 (2016) 3814–3826. doi:10.1021/acs.jced.6b00451.

[4] M. Li, M. Lai, Solubility and Diffusivity of N_2O and CO_2 in (Monoethanolamine plus N-Methlydiethanolamine plus Water) and in (Monoethanolamine plus 2-Amino-2-Methyl-1-Propanol plus Water), J. Chem. Eng. Data 40 (1995) 486–492. doi:10.1021/je00018a029.

[5] B. Rumpf, G. Maurer, An Experimental and Theoretical Investigation on the Solubility of Carbon Dioxide in Aqueous Solutions of Strong Electrolytes, Ber. Bunsenges. Phys. Chem. 97 (1993) 85–97. doi:10.1002/bbpc.19930970116.

[6] A. Penttilä, C. Dell'Era, P. Uusi-Kyyny, V. Alopaeus, The Henry's Law

Constant of N_2O and CO_2 in Aqueous Binary and Ternary Amine Solutions (MEA, DEA, DIPA, MDEA, and AMP), Fluid Phase Equilib. 311 (2011) 59–66. doi:10.1016/j.fluid.2011.08.019.

[7] K. Wissbrun, D. French, A. Patterson, The True Ionization Constant of Carbonic Acids in Aqueous Solution from 5 Degrees to 45 Degrees, J. Phys. Chem. 58 (1954) 693–695. doi:10.1021/j150519a004.

[8] A. Ellis, The Effect of Pressure on the First Dissociation Constant of Carbonic Acid, J. Chem. Soc. 4 (1959) 3689–3699. doi:10.1039/jr9590003689.

[9] R. Crovetto, Evaluation of Solubility Data of the System CO_2-H_2O from 273 K to the Critical Point of Water, J. Phys. Chem. Ref. Data 20 (1991) 575–589. doi:10.1063/1.555905.

[10] G. Versteeg, W. van Swaaij, Solubility and Diffusivity of Acid Gases (CO_2, N_2O) in Aqueous Alkanolamine Solutions, J. Chem. Eng. Data 33 (1988) 29–34. doi:10.1021/je00051a011.

[11] G. Browning, R. Weiland, Physical Solubility of Carbon-Dioxide in Aqueous Alkanolamines via Nitrous-Oxide Analogy, J. Chem. Eng. Data 39 (1994) 817–822. doi:10.1021/je00016a040.

[12] L. Pauling, The Nature of the Chemical Bond, Third Edition, Cornell University Press, Ithaca, New York, 1960.

[13] R. Span, W. Wagner, A New Equation of State for Carbon Dioxide Covering the Fluid Region from the Triple-point Temperature to 1100 K at Pressures up to 800 MPa, J. Phys. Chem. Ref. Data 25 (1996) 1509–1596. doi:10.1063/1.555991.

[14] E. Lemmon, R. Span, Short Fundamental Equations of State for 20 Industrial Fluids, J. Chem. Eng. Data 51 (3) (2006) 785–850. doi:10.1021/je050186n.

[15] W. Kunerth, Solubility of CO_2 and N_2O in Certain Solvents, Phys. Rev. 19 (1922) 512–524. doi:10.1103/PhysRev.19.512.

[16] M. Postigo, M. Katz, Solubility and Thermodynamics of Carbon Dioxide in Aqueous Ethanol Solutions, J. Solution Chem. 16 (1987) 1015–1024. doi:10.1007/BF00652585.

[17] I. Dalmolin, E. Skovroinski, A. Biasi, M. L. Corazza, C. Dariva, J. V. Oliveira, Solubility of Carbon Dioxide in Binary and Ternary Mixtures with Ethanol and Water, Fluid Phase Equilib. 245 (2006) 193–200. doi:10.1016/j.fluid.2006.04.017.

[18] M. Lisal, W. Smith, K. Aim, Analysis of Henry's Constant for Carbon Dioxide in Water via Monte Carlo Simulation, Fluid Phase Equilib. 226 (2004) 161–172. doi:10.1016/j.fluid.2004.06.062.

[19] E. Cichowski, T. Schmidt, J. Errington, Determination of Henry's Law Constants through Transition Matrix Monte Carlo Simulation, Fluid Phase Equilib. 236 (2005) 58–65. doi:10.1016/j.fluid.2005.05.001.

[20] T. Schnabel, J. Vrabec, H. Hasse, Henry's Law Constants of Methane, Nitrogen, Oxygen and Carbon Dioxide in Ethanol from 273 to 498 K: Prediction from Molecular Simulation, Fluid Phase Equilib. 233 (2005) 134–143. doi:10.1016/j.fluid.2005.04.016.

[21] L. Zhang, J. Siepmann, Direct Calculation of Henry's Law Constants from Gibbs Ensemble Monte Carlo Simulations: Nitrogen, Oxygen, Carbon Dioxide and Methane in Ethanol, Theor. Chem. Acc. 115 (2006) 391–397. doi:10.1007/s00214-005-0073-1.

[22] T. Merker, J. Vrabec, H. Hasse, Molecular Simulation Study on the Solubility of Carbon Dioxide in Mixtures of Cyclohexane+Cyclohexanone, Fluid Phase Equilib. 315 (2012) 77–83. doi:10.1016/j.fluid.2011.11.003.

[23] T. Merker, J. Vrabec, H. Hasse, Gas Solubility of Carbon Dioxide and

of Oxygen in Cyclohexanol by Experiment and Molecular Simulation, J. Chem. Thermodyn. 49 (2012) 114–118. doi:10.1016/j.jct.2012.01.017.

[24] T. Merker, C.-M. Hsieh, S.-T. Lin, H. Hasse, J. Vrabec, Fluid-phase Coexistence for the Oxidation of CO_2 Expanded Cyclohexane: Experiment, Molecular Simulation, and COSMO-SAC, AIChE J. 59 (2013) 2236–2250. doi:10.1002/aic.13986.

[25] Q. Chen, S. Balaji, M. Ramdin, J. Gutierrez-Sevillano, A. Bardow, E. Goetheer, T. Vlugt, Validation of the CO_2/N_2O Analogy Using Molecular Simulation, Ind. Eng. Chem. Res. 53 (2014) 18081–18090. doi:10.1021/ie503488n.

[26] H. Jiang, O. Moultos, I. Economou, A. Panagiotopoulos, Gaussian-Charge Polarizable and Nonpolarizable Models for CO_2, J. Phys. Chem. B 120 (2016) 984–994. doi:10.1021/acs.jpcb.5b11701.

[27] M. Costa Gomes, J. Deschamps, A. Padua, Interactions of Nitrous Oxide with Fluorinated Liquids, J. Phys. Chem. B 110 (2006) 18566–72. doi:10.1021/jp062995z.

[28] N. Hansen, F. Agbor, F. Keil, New Force Fields for Nitrous Oxide and

Oxygen and their Application to Phase Equilibria Simulations, Fluid Phase Equilib. 259 (2007) 180–188. doi:10.1016/j.fluid.2007.07.014.

[29] V. Lachet, B. Creton, T. de Bruin, E. Bourasseau, N. Desbiens, O. Wilhelmsen, M. Hammer, Equilibrium and Transport Properties of CO_2+N_2O and CO_2+NO Mixtures: Molecular Simulation and Equation of State Modelling Study, Fluid Phase Equilib. 322 (2012) 66–78. doi:10.1016/j.fluid.2012.03.011.

[30] C. G. Gray, K. E. Gubbins, Theory of Molecular Fluids, Vol. 1: Fundamentals, Clarendon Press, Oxford, 1984.

[31] H. Lorentz, Ueber die Anwendung des Satzes vom Virial in der kinetischen Theorie der Gase, Ann. Phys. 248 (1881) 127–136.

[32] D. Berthelot, Sur le melange des gaz, Comptes Rendus de l'Academie des Sciences Paris 126 (1898) 1703–1706, 1857–1858.

[33] J. Abascal, C. Vega, A General Purpose Model for the Condensed Phases of Water: TIP4P/2005, J. Chem. Phys. 123 (2005) 234505–1–234505–12. doi:10.1063/1.2121687.

[34] C. Vega, J. Abascal, Simulating Water with Rigid Non-polarizable Mod-

els: A General Perspective, Phys. Chem. Chem. Phys 13 (2011) 19663–19688. doi:10.1039/c1cp22168j.

[35] S. Reiser, N. McCann, M. Horsch, H. Hasse, Hydrogen Bonding of Ethanol in Supercritical Mixtures with CO_2 by ^{1}H NMR Spectroscopy and Molecular Simulation, J. Supercrit. Fluids 68 (2012) 94–103. doi:10.1016/j.supflu.2012.04.014.

[36] S. Miroshnichenko, J. Vrabec, Excess Properties of Non-ideal Binary Mixtures Containing Water, Methanol and Ethanol by Molecular Simulation, J. Mol. Liq. 212 (2015) 90–95. doi:10.1016/j.molliq.2015.08.058.

[37] S. Reiser, M. Horsch, H. Hasse, Density of Ethanolic Alkali Halide Salt Solutions by Experiment and Molecular Simulation, Fluid Phase Equilib. 408 (2016) 141–150. doi:10.1016/j.fluid.2015.08.005.

[38] G. Guevara-Carrion, T. Janzen, Y. Munoz-Munoz, J. Vrabec, Mutual Diffusion of Binary Liquid Mixtures Containing Methanol, Ethanol, Acetone, Benzene, Cyclohexane, Toluene, and Carbon Tetrachloride, J. Chem. Phys. 144 (2016) 124501–1–124501–23. doi:10.1063/1.4943395.

[39] J. Vrabec, J. Stoll, H. Hasse, A Set of Molecular Models for Symmet-

ric Quadrupolar Fluids, J. Phys. Chem. B 105 (2001) 12126–12133. doi:10.1021/jp012542o.

[40] T. Merker, C. Engin, J. Vrabec, H. Hasse, Molecular Model for Carbon Dioxide Optimized to Vapor-liquid Equilibria, J. Chem. Phys. 132 (2010) 234512–1–234512–7. doi:10.1063/1.3434530.

[41] J. Stoll, J. Vrabec, H. Hasse, J. Fischer, Comprehensive Study of the Vapour-liquid Equilibria of the Pure Two-centre Lennard-Jones plus Pointquadrupole Fluid, Fluid Phase Equilib. 179 (2001) 339–362. doi:10.1016/S0378-3812(00)00506-9.

[42] K. Stöbener, P. Klein, M. Horsch, K. Küfer, H. Hasse, Parametrization of Two-center Lennard-Jones plus Point-Quadrupole Force Field Models by Multicriteria Optimization, Fluid Phase Equilib. 411 (2016) 33–42. doi:10.1016/j.fluid.2015.11.028.

[43] T. Merker, J. Vrabec, H. Hasse, Engineering Molecular Models: Efficient Parameterization Procedure and Cyclohexanol as Case Study, Soft Mater. 10 (2012) 3–25. doi:10.1080/1539445X.2011.599695.

[44] B. Eckl, J. Vrabec, H. Hasse, An Optimised Molecular Model for Ammonia, Mol. Phys. 106 (2008) 1039–1046. doi:10.1080/00268970802112137.

[45] J. Vrabec, H. Hasse, Grand Equilibrium: Vapour-liquid Equilibria by a New Molecular Simulation Method, Mol. Phys. 100 (2002) 3375–3383. doi:10.1080/00268970210153772.

[46] S. Werth, S. Lishchuk, M. Horsch, H. Hasse, The Influence of the Liquid Slab Thickness on the Planar Vapor-liquid Interfacial Tension, Physica A 392 (2013) 2359–2367. doi:10.1016/j.physa.2013.01.048.

[47] K. Shing, K. Gubbins, K. Lucas, Henry Constants in Non-Ideal Fluid Mixtures: Computer Simulation and Theory, Mol. Phys. 65 (1988) 1235–1252. doi:10.1080/00268978800101731.

[48] H. Flyvbjerg, H. Petersen, Error-estimates on Averages of Correlated Data, J. Chem. Phys. 91 (1989) 461–466. doi:10.1063/1.457480.

[49] C. W. Glass, S. Reiser, G. Rutkai, S. Deublein, A. Köster, G. Guevara-Carrion, A. Wafai, M. Horsch, M. Bernreuther, T. Windmann, H. Hasse, J. Vrabec, ms2: A Molecular Simulation Tool for Thermodynamic Properties, New Version Release, Comput. Phys. Commun. 185 (2014) 3302–3306. doi:10.1016/j.cpc.2014.07.012.

[50] C. Niethammer, S. Becker, M. Bernreuther, M. Buchholz, W. Eckhardt, A. Heinecke, S. Werth, H.-J. Bungartz, C. Glass, H. Hasse, J. Vrabec,

M. Horsch, ls1 mardyn: The Massively Parallel Molecular Dynamics Code for Large Systems, J. Chem. Theory Comput. 10 (2014) 4455–4464. doi:10.1021/ct500169q.

[51] A. Lotfi, J. Vrabec, J. Fischer, Vapor-liquid Equilibria of the Lennard-Jones Fluid from the NPT plus Test Particle Method, Mol. Phys. 76 (1992) 1319–1333. doi:10.1080/00268979200102111.

[52] R. Rowley, W. Wilding, J. Oscarson, Y. Yang, N. Zundel, T. Daubert, R. Danner, DIPPR Information and Data Evaluation Manager for the Design Institute for Physical Properties, Version 7.0.0, AIChE, 2013.

[53] S. Werth, K. Stöbener, P. Klein, K. Küfer, M. Horsch, H. Hasse, Molecular Modelling and Simulation of the Surface Tension of Real Quadrupolar Fluids, Chem. Eng. Sci. 121 (2015) 110–117. doi:10.1016/j.ces.2014.08.035.

[54] J. Barker, R. Watts, Monte Carlo Studies of Dielectric Properties of Water-like Models, Mol. Phys. 26 (1973) 789–792. doi:10.1080/00268977300102101.